Rare Metal Materials and Engineering
Volume 48, Issue 1, January 2019
Available online at www.rmme.ac.cn

Science Press

Cite this article as: Rare Metal Materials and Engineering, 2019, 48(1): 0044-0054.

ARTICLE

Review on Joining Process of Carbon Fiber-reinforced Polymer and Metal: Applications and Outlook

Zhang Dawei[1], Zhang Qi[1], Fan Xiaoguang[2], Zhao Shengdun[1]

[1] Key Laboratory of Education Ministry for Modern Design and Rotor-Bearing System, Xi'an Jiaotong University, Xi'an 710049, China; [2] State Key Laboratory of Solidification Processing, Northwestern Polytechnical University, Xi'an 710072, China

Abstract: The hybrid structure of composite material such as carbon fiber-reinforced polymer (CFRP) and metal such as steel, aluminum alloy or titanium alloy is an effective structure to realize lightweight with reliable structural strength. The CFRP-metal hybrid structure is widely used in aircraft, automobile and watercraft. The CFRP-metal joints joined by plastic deformation are characterized by lightweight and high-strength, which are suitable for various working environments. Thus, the advanced joining method based on plastic deformation has a good application prospect. The application of various joining techniques between CFRP and metal, as well as the strength of hybrid joints, was reviewed. Some future researches and developments of CFRP-metal hybrid joints with high-performance, light-weight and high-reliability were highlighted.

Key words: carbon fiber-reinforced polymer; aluminum alloy; steel; titanium alloy; niobium alloy; strength of joint

The production of carbon fiber-reinforced polymer (CFRP) and the use of CFRP in new generation of aircraft both have increased sharply[1-5]. However, metals such as titanium alloy, aluminum alloy and steel will still be used in aircraft, automobiles and watercraft for the foreseeable future. The hybrid structure of composite material and metal can effectively reduce the weight, and is widely used. Thus, CFRP-metal joining process plays an important role in the development of aircraft, automobile and watercraft industries.

The joint of various metals to CFRP and the working environment of CFRP-metal hybrid joints place some critical demands for the joining process of CFRP to metal. Lots of joining methods, such as adhesive bonding, bolt connection, riveting, welding, "z-pin" (pin inserts), and joining (such as self-pierce riveting, hot riveting, mechanical clinching, friction welding) by plastic deformation, have been used to join CFRP to metal. Ref. [6] has reviewed these joining methods and their process for CFRP-metal. However, the application scope of CFRP-metal hybrid structure is determined by the performance (such as strength) of hybrid joints, especially in the working environment. For example, the strength of a hybrid joint by adhesive bonding (AB) will rapidly degrade[7], and the damage evolutions of hybrid joints under thermal load are different for different riveting processes[8].

Thus, based on Ref.[6], the successful application cases and evaluation of CFRP-metal hybrid joint were further reviewed in the present study. It focuses mainly on the "z-pin" (pin inserts), welding, and joining by plastic deformation. Finally, some systematical studies for developing CFRP-metal joining techniques were highlighted.

1 Estimating Method of Strength

Quasi-static tensile test and fatigue test are the main experimental methods for estimating the strength of the joint, and there are a lot of test standards and various indicators. Among them, the quasi-static tensile test is the most commonly used test and is reported most in the academic literature. In general, tensile shear strength of joints can be calculated by the following expression:

Received date: December 25, 2017
Foundation item: National Natural Science Foundation of China (51675414); Fund of the State Key Laboratory of Solidification Processing in NWPU (SKLSP201623)
Corresponding author: Zhang Dawei, Ph. D., Associate Professor, School of Mechanical Engineering, Xi'an Jiaotong University, Xi'an 710049, P. R. China, Tel: 0086-29-82668607, E-mail: zhangdawei2000@mail.xjtu.edu.cn

$$\tau = \frac{F_{\mathrm{UT}}}{A} \quad (1)$$

where τ is the tensile shear strength; F_{UT} is the ultimate tensile force; A is the joining area.

F_{UT} is the direct index for measuring the strength of CFRP-metal hybrid joints. The tensile strength τ is an index after data processing. However, for different joining methods, the calculation of area A is different. In the same process, the calculations are even different, especially for the joining processes with CFRP melting.

Thus, the tensile strength (τ or F_{UT}) of CFRP-metal hybrid joint is summarized in Appendix A. The detailed evaluation of the strength of CFRP-metal hybrid joint will be described in the next section.

2 Application and Evaluation of Joining Process of CFRP-Metal Hybrid Joint

2.1 Adhesive bonding

Adhesive bonding has been widely used for material joining, and it is suitable for almost all materials, although AB needs careful surface treatment and a long cured time. However, the strength of adhesively bonded joint is sensitive to the working environment and adhesive properties. The strength of bonded joint will quickly degenerate under severe conditions, especially under hydrothermal condition [9,10]. The strength of joint is also reduced when the materials are exposed to moisture before bonding[9].

Generally, the thermal expansion coefficients of CFRP and metal (such as aluminum alloy) present a notable difference. Thus, the residual tensile stress appearances in aluminum alloy plate in CFRP-aluminum alloy joint due to greater thermal expansion coefficient, which will reduce the performance of joint[11].

One racing car suspension consisting of CFRP tube and aluminum alloy bar was joined by ultrasonic vibration-assisted adhesive bonding (UVAB), and the strength of hybrid joint increase by 52% under the optimal scheme obtained from an orthogonal experiment[12,13]. The vibration position and time have a significant influence on the strength, and the ultrasonic vibration exerted along the axial direction can obtain a maximal improvement for strength [12,13]. The axial ultrasonic vibration is difficult to load for long car suspension part or joining between plates. Thus, the ultrasonic vibration exerted along the radial direction (such as position 1, 2, 3 shown in Fig. 1) was adopted in practice, and the strength of joint increase by 40% under the optimal scheme[12,13].

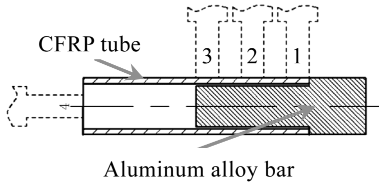

Fig. 1 Vibration position[13]

2.2 Mechanical fastening

There are more abundant and comprehensive experimental and numerical studies of the strength and failure of composite-composite joint by mechanical fastening[14-18]. The plastic deformation exerts around the pre-hole before the failure of the metal-metal joint by mechanical fastening, but there is no plastic deformation for composite-composite joint due to the brittle composite material [19]. The failure model of composite-metal joint is different from the failure of composite-composite or metal-metal joint. In mechanical fastening process of CFRP and metal, titanium alloy or aluminum alloy bolts/rivets are also used beside the steel bolts/rivets. The failure model of CFRP-metal hybrid joint shows a difference if bolts/rivets of different materials are used.

The composite-metal joint is also susceptible to bolt load loss under creep and environmental effect[20,21]. Caccese et al[20] developed a monitoring system for bolt load loss in composite-metal joint to reduce maintenance cost. The bolt load loss in the bolted joint between CFRP and aluminum alloy was also studied by creep compression tests[21]. The results indicate that the relaxation of the material is determined by temperature and pressure, and the improvement of surface quality of CFRP sheet can reduce load loss.

The influence of bolt-hole clearance on the composite-composite joint has been investigated by McCarthy et al[22], and the results indicated that the clearance has little effect on the quasi-static strength and has a significant effect on fatigue life. However, the research[23,24] of the influence of interference fit on CFRP-titanium alloy indicated that the quasi-static strength increases first and then decrease with increasing interference fit, and the best interference fit considering fatigue life is determined by the cyclic stress level.

Fiore et al[7] investigated the influence of salt spray fog on the composite-aluminum alloy joints by experiments according to the ASTM B 117 standard. The strength of joint notably decreases with the increasing aging time of salt-fog exposure. Compared with unaged joints, the maximum tensile load of CFRP-aluminum alloy joints decrease by 23% after aging 7 weeks and 31.4% after aging 15 weeks. The degradation sensitivity of CFRP-metal joint in the salt-fog environment is lower than that of glass fiber-reinforced polymer-metal joint.

Marannano et al [25] declared that material of rivet has an influence on the failure model of CFRP-aluminum alloy joint by quasi-static stretching, which are flexural deformation of steel rivet and shear failure of aluminum

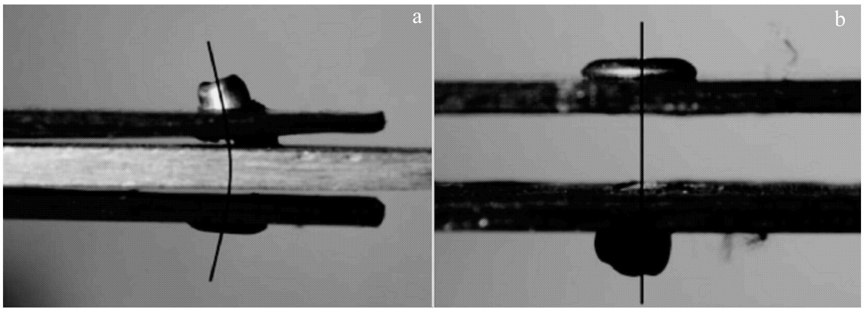

Fig.2 Failure mode of riveted CFRP-aluminum alloy joint with different rivets[25]: (a) steel rivet and (b) aluminum alloy rivet

alloy rivet, as shown in Fig. 2. The failure model of riveted-bonded joint also shows difference between the uses of different rivets. Steel rivet is responsible for the joint failure caused by rivet bending and bearing failure of CFRP, and aluminum alloy rivet is responsible for adhesive failure and rivet shearing failure[25].

The static tensile strength of CFRP-aluminum alloy joints by bonding and riveting increases by at least 20% compared with that of simple bonded or riveted joints[25]. However, the fatigue strength of joints riveted by different rivets shows difference. The low and high cycle fatigue of hybrid joint using steel rivet are both improved by bonded combing riveting, but only low cycle fatigue is improved for using aluminum alloy rivet[25].

Compared with conventionally riveted joint of CFRP to titanium alloy, the fatigue life of joint by rivet combining adhesive bonding or bolt combining surface structure (Fig. 5b in Ref.[6]) of metal sheet will be improved[26]. The laser riveted (LR) joint (Fig.5a in Ref.[6]) of CFRP to Ti-6Al-4V has a higher stiffness with plane surface and low weight[26].

The strength of joints is not always improved by the hybrid jointing method combining mechanical fastening and adhesive bonding. Kweon et al[27] proposed that the strength of bolted-bonded joints of CFRP to aluminum alloy will only be improved when mechanical fastening is stronger than adhesive bonding in the bolted-bonded joint.

2.3 Joining by “z-pin”

Tensile tests of CFRP-metal joint indicated that the stiffness decreases after maximal force[28]. The failure of CFRP-metal joint is caused by shear and bending deformation of the inserted pin and micro cracks of CFRP, as shown in Fig.3, and the inserted pin may fracture[28].

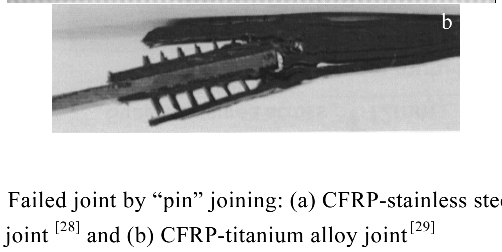

Fig.3 Failed joint by “pin” joining: (a) CFRP-stainless steel joint [28] and (b) CFRP-titanium alloy joint[29]

Compared with pins attached by electron beam melting (EBM), the pin welding by cold metal transfer (CMT) has a large load bearing capacity[29]. However, the geometric features of pins attached by EBM are more controllable. The shape of pin and the shape of metal in joining region play an important role in the tensile strength of the joint. The wedge pin has a higher failure load[30] and the scarfed insert has a larger load bearing capability[31]. The difference in failure load of joint with different shapes of pins ranges from 36% to 114% [32, 33].

The reinforced joint by pin has a remarkable advantage in maximal tension force, local strain at the maximal force (increase 470% to 1000%), and energy absorption capacity compared with the adhesively bonded joint (i.e. co-cured joint)[28], and the maximal tension force can increase 124% by suitable shapes of the pin and the inserted metal in joining region[31].

2.4 Welding

Static tensile test of brazed joints of CFRP and titanium alloy or niobium alloy indicated that shear fracture occurs in CFRP and the strength of the hybrid joint is larger than the strength of CFRP[34].

Strength of joint by resistance welding (RW) is determined by processing parameters such as power, pressure and welding time. Incomplete filling of micro-porosity on the aluminum alloy substrate was caused by short welding time, and the thermal degradation was caused by the long welding time, while both aspects will reduce the strength of welding joint[35].

The surface pre-treatment plays an important role in the strength of joint by induction heated joining (IHJ)[36]. Experiment results indicate that the shear tensile strength is increased by a higher surface roughness and acidic pickling. An additional polymer film between the two partners leads to a higher bonding strength of the joint and the joining pressure also contributes to the strength of CFRP-metal hybrid joint[36].

A suitable heat treatment before ultrasonic welding (UW) increases the surface roughness, and then increases the tensile shear strength of CFRP-aluminum alloy joint[37]. The failure of hybrid joint by ultrasonic welding often occurs in the actual welding (i.e. bonding) zone, as shown in Fig.4[38].

Failure of CFRP-steel joint by laser joining (LJ) occurs at the connection interface [39,40], but failure of hybrid joint between CFRP and Cr or Zn-coated steel occurs inside the CFRP under interface[39, 41]. Many bubbles are generated inside the melted area during laser joining process, and mechanical properties of hybrid joint will be reduced by large numbers and large sizes of bubbles [40,42-44]. Tan et al [45] studied the formation mechanism of bubble during laser joining process of CFRP-steel joint, and concluded that two types of bubbles in CFRP can be generated, one of which occurs depending on the heat input and the other type is generated under all experimental conditions.

The laser Surfi-Sculpt was introduced into the surface pre-treatment of aluminum alloy before laser joining[46]. The tensile shear strength of CFRP-aluminum alloy joint increases by 459%, as shown in Fig. 5.

2.5 Joining by plastic deformation Application of the model

2.5.1 Self-pierce riveting

The influences of thermal load (from 23°C to 180°C) on the CFRP-steel joint by blind riveting (BR) and self-pierce riveting (SPR) processes were investigated by Wagner et al[8]. The damage evolution is determined by the internal stresses caused by different thermal expansion behaviors and initial characteristics of riveting in different riveting processes. The influence of thermal load on the damage by blind riveting is notably greater than that by SRP, as shown in Fig. 6. The initial size of damage caused by SPR is larger than that caused by blind riveting, but the evolution is homogenous and the longitudinal scatter is not more notable compared to blind riveting. The shear tension tests after thermal load indicate that the strengths reduce but failures for blind riveting and SPR are different [8]. Bearing failure and rivet pull-out failure are caused by blind riveting and SPR, respectively.

Fracture model of hybrid joint of CFRP and aluminum alloy is determined by the relative position of material[47]. The tensile experiment of hybrid joint by friction stir blind riveting (FSBR) indicated that fracture occurs in CFRP sheet when CFRP is placed at the bottom, and rivet slips in metal sheet when aluminum alloy is placed at the bottom, as shown in Fig.7. The strength of the latter hybrid joint will be larger than the strength of the former.

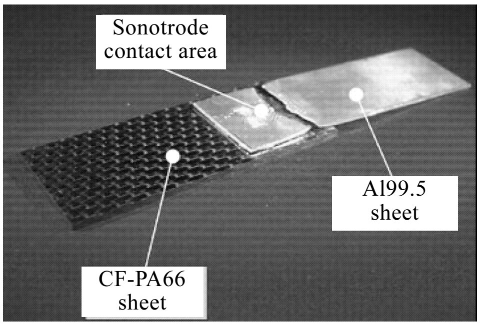

Fig.4 Failure of CFRP-aluminum joint by ultrasonic welding[38]

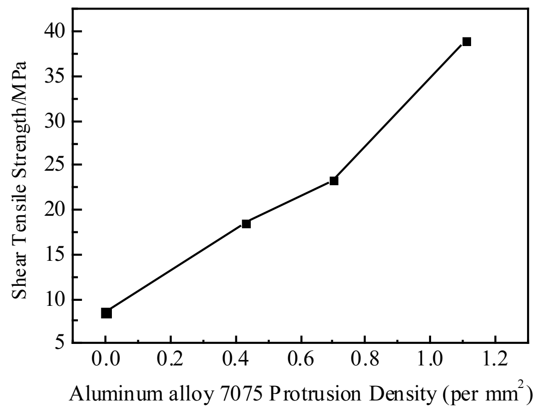

Fig.5 Tensile shear strength of CFRP-aluminum alloy joint by laser joining[46]

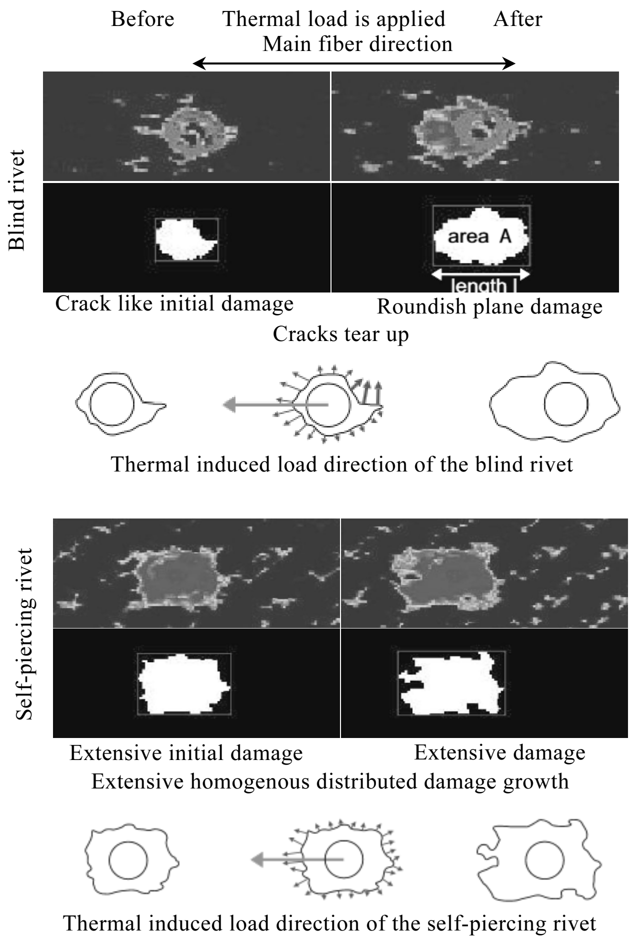

Fig.6 Damage around riveting point by C-scan[8]

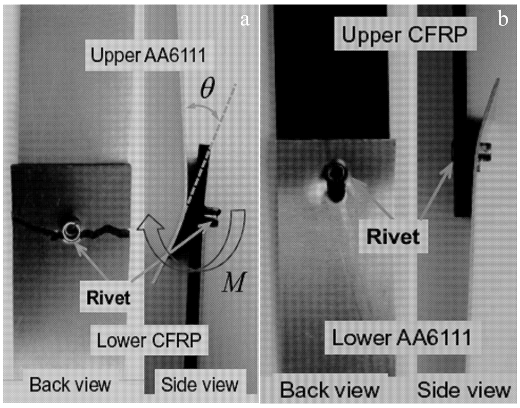

Fig. 7 Fractured joint by FSBR[47]: (a) CFRP at bottom and (b) CFRP at top

The resistance level of SPR-bonded joint between CFRP and aluminum alloy is determined by bonding and the failure energy of the SPR-bonded joint is determined by SPR [48]. The study indicated that the tensile strength of hybrid SPR-bonded joint increases by 13% to 32% and the stiffness of hybrid joint increases by 7% to 25% according to CFRP lay-up and heat treating (post-curing treatment, i.e. 100 °C for 3 h) for bonding. The failure of the hybrid joint occurs after adhesive failure, and then fracture occurs in cross-ply CFRP ([(0°/90°)]) and rivet is pulled out for angle-ply CFRP ($[(0°/90°/(+45°)_2)]_S$)[48].

2.5.2 Hot riveting

The shear tension tests of CFRP-AA2024 hybrid joint by hot riveting (HR) indicated that shear strength of joint increases with increasing joining temperature (Fig. 8)[49].

Under-filling of hole cavities will cause a low joining temperature, as shown in Fig. 9a, and the better cavity fill will be obtained at a suitable high temperature, as shown in Fig. 9b. These lead to a difference in shear tensile strength of hybrid joint, and the fracture model of hybrid joint also differs. The pull-out failure occurs for the HR hybrid joint at a low joining temperature, as shown in Fig. 9c, and the fracture occurs for the HR hybrid joint at the high temperature, as shown in Fig. 9d.

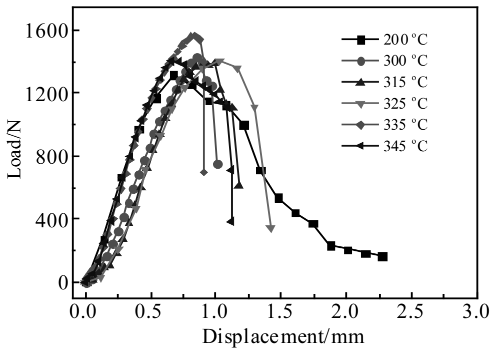

Fig. 8 Load-displacement curves during tensile test of hybrid joints by hot riveting [49]

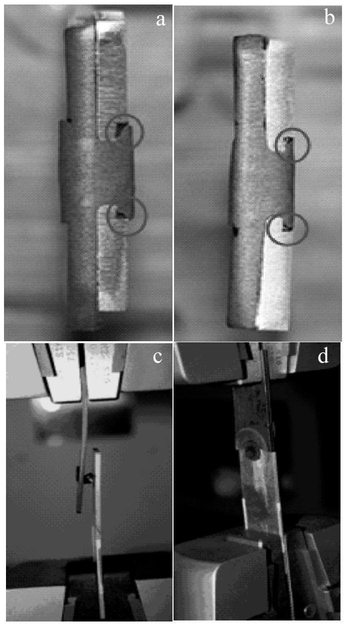

Fig. 9 Filling and failure of joints by hot riveting: (a) cross-section at 200 °C, (b) cross-section at 335 °C, (c) pull-out at 200 °C, and (d) fracture at 335°C

2.5.3 Mechanical clinching

In order to improve formability of CFRP, a dummy metal sheet is introduced into the mechanical clinching (MC). Compared with the clinched-bonded joint with dummy, the shear tensile strength of clinched-bonded joint without dummy sheet dropped sharply, and the brittle crack was found on the surface of quasi-isotropic lay-up ([0º/60º/120º/60º/0º])[50]. If the relative position of CFRP changes, i.e. dummy sheet-CFRP-adhesive-metal from the punch to the lower die, the shear tensile strength also drops sharply due to the small degree of deformation [50].

The strength of CFRP-AA2017 joint by clinching-bonding process is also larger than that by rivet-bonding or adhesive bonding method[50]. Compared with the adhesively bonded joint, the shear tensile strength of CRFP-metal joint obtained from an optimal clinching-bonding process increases by 69.2% and 89.3% for cross lay-up CFRP ([0º/90º/0º/0º/90º/0º]) and quasi-isotropic lay-up CFRP, respectively. However, experiments indicated that there is notable delamination in the quasi-isotropic lay-up CFRP of the hybrid joint, as shown in Fig. 10d.

In two-steps clinching process, i.e. mechanical clinching with reshaping (MCR), the clinched joint was reshaped, and the reshaping force is mainly exerted on the metal side-wall (such as aluminum alloy) of CFRP-metal joint[51]. The neck thickness and undercut thickness are the key parameters to evaluate quality of clinching joint[52]. The neck thickness and undercut thickness of CFRP-AA6024 can be improved under suitable reshaping depth and force[51], as shown in

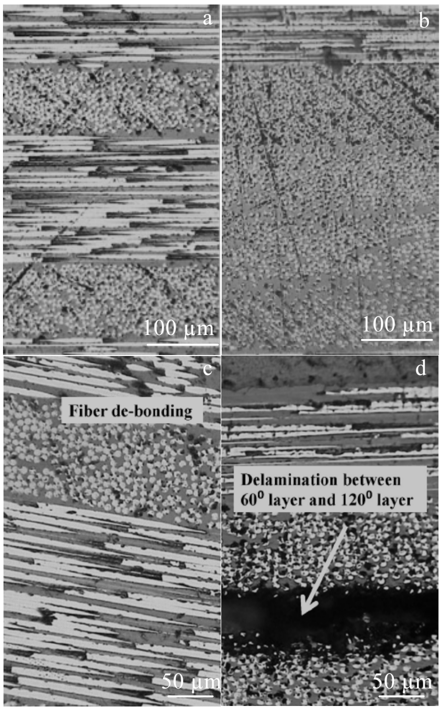

Fig.10 Cross-section of CFRP[50]: (a) cross lay-up CFRP before clinching, (b) quasi-isotropic lay-up CFRP before clinching, (c) cross lay-up CFRP after clinching, (d) quasi-isotropic lay-up CFRP after clinching

Fig.11, and thus the strength of hybrid joint can be increased by this two-steps clinching process. The shear test indicated that the shear strength of reshaped joint can increase by 32% under suitable reshaping conditions and the strength may reduce under improper reshaping conditions.

The shear tensile strength of CRFP-steel joint by hole-(mechanical)-clinching (HMC) depends on the diameter of punch, and the strength increases in proportion to the diameter but excessive diameter will reduce the strength[53] , as shown in Fig.12. The shear test indicated that the failure of hole-clinched joint is button separation with CFRP fracture at a suitable punch diameter and is metal neck fracture at an excessive diameter.

2.5.4 Friction welding

The surface treatment of aluminum alloy before friction lap welding (FLW) and the rotation and joining speeds in

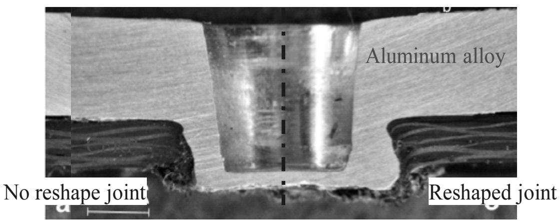

Fig.11 Comparison of geometry of clinched joint[51]

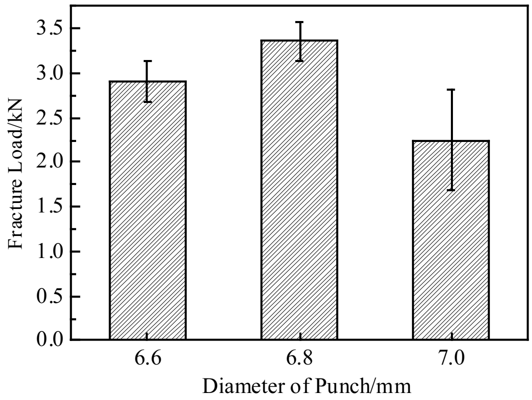

Fig.12 Strength and failure modes of hole-clinched joint[53]

FLW play the important roles in strength and fracture model[54, 55]. The hydroxide $Al(OH)_3$ is generated on the surface of aluminum alloy sheet during grinding treatment, and the hydroxide $Al(OH)_3$ strongly contributes to interfacial wetting between molten polymer and aluminum alloy. Thus the tensile shear strength increases notably for the friction lap welded joint of CFRP and aluminum alloy with grinding treatment [54]. The tensile shear strength of hybrid joint by FLW increases at first and then decreases with increasing tool rotation speed or joining speed[54,55].

The fracture surface of hybrid joint by FLW in tool-passed zone on metal side can be classified into fractured models [54, 55]: joint interface fracture, CFRP void fracture and CFRP-itself fracture, as shown in Fig.13. The void in CFRP generated during FLW is not the main factor in determining the strength of hybrid joint. CFRP-itself fracture plays a leading role under low joining speed and interface fracture plays a leading role under high joining speed [54]. However, interface fracture dominates under low rotation speeds[55].

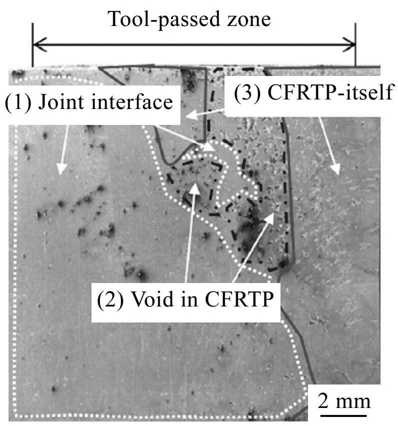

Fig.13 Fractured surface characteristics of CFRP-AA5052 joint by FLW[54]

The surface treatment of aluminum alloy before friction spot welding (FSpW) also improves the tensile shear strength of CFRP-aluminum alloy joint. Pure aluminum coated layer increases the deformation capacity and volume of polymer attached to the metal surface, and increasing roughness (R_a=2~4.5 μm) also increases the mechanical interlock and adhesive force, and these ways increase the shear strength by at least 80% and 17%, respectively[56]. Increasing the rotation speed and plunge depth of FSpW can increase the contact between CFRP and metal, and then the shear strength of hybrid joint will be improved[56]. By optimizing the process parameters such as rotation speed, plunge depth, joining time and joining force, the ultimate shear force of CFRP-AA6181 joint by FSpW increases from 2107 N to 3523 N[57].

The polymer in CFRP contributes greatly to micro-mechanical interlock and adhesion force of hybrid joint. Thus, a polymer film was added between CFRP and metal before friction joining. Compared with the hybrid joint by FSpW without film, the ultimate shear force of hybrid joint by FSpW with film increases by 55% under low heat input and 20% under high heat input[58], where the heat input is determined by the rotation speed of tool.

3 Conclusions and Outlook

The adhesive bonding and mechanical fastening are suitable for joining CFRP to almost all metals. But the joint is sensitive to working environment or adds weight sharply. The welding is suitable for joining CFRP to hard-to-deform metal such as titanium alloy, aluminum alloy 7XXX, but an additional polymer film or metal film may need to increase strength or achieve welding. The joining by plastic deformation is suitable for joining CFRP to metal with well plastic at room temperature, such as aluminum alloy 2XXX, 6XXX.

The joining by plastic deformation, such as hot riveting, has a good potential to reduce mass and avoid corrosion. The strength of CFRP-metal can be improved by optimizing the processing parameters and improving the joining process. However, the performance of CFRP is very different from that of metal. The plastic deformation couples the welding features during the joining process, and thus the deformation boundary is very complex. Then, it is difficult to understand the mechanism of joining process, and to optimize processing parameters and to control the process. Therefore, the following aspects are needed to systematically research for developing CFRP-metal joining technique.

1) To analyze the relationship between polymer flow and fiber flow during the formation of CFRP, and then to model suitable constitutive equation of CFRP. To develop an efficient and accurate finite element model which can describe the deformation characteristics of the polymer and fiber and the welding/bonding characteristics on the interface between CFRP and metal.

2) The failure model of CFRP-metal joint has a notable difference for different joining processes. Even by the same joining process, the failure/fracture is affected by processing parameters and partner structures such as shape of pins in “z-pin” joining, relative position of metal sheets in SPR, joining temperature in hot riveting. Thus, there is an urgent need to understand the failure mechanism of CFRP-metal joint.

3) To research the joining process characteristics of CFRP-metal hybrid joint by various joining processes, especially by plastic deformation under complex joining conditions. To establish a application scope of various joining processes for joining types (such as fiber content, short or long fiber, resin type) of CFRP and metal system.

4) To optimize and control the joining process by plastic deformation. Understand the influences of material parameters, geometry parameters and processing parameters on the joining process and strength of CFRP-metal hybrid joints. To achieve the coordinated control of joining process and joint strength by controlling the controllable parameters.

Appendix A: Table 1

Table 1 Static tensile strength of CFRP-metal hybrid joint

Joining process	Joining material		S: Surface treatment; A: Adhesive; B(R): Material of bolt (rivet)	Strength of hybrid joint, F_{UT}/τ	Remark	Ref.
	CFRP	Metal				
BR	[±45°]$_s$ (2.1 mm)	Steel CR240BH (1.5 mm)	-	13160 N	-	[8]
SPR			-	13460 N	-	[8]
BR			-	11860 N	Heating joint for 20 min at 180 °C	[8]
SPR			-	11690 N		[8]
HMC	53 vol% woven fibers (1.2 mm)	Steel SPRC440 (1.6 mm)	-	2250~3360 N	-	[53]
z-pin	Thermoset CFRP	Stainless steel 304	-	23900~32850 N	-	[28]

Continued table

LJ	30 vol% short fibers (3 mm)	Mild steel (1.2 mm)	-	2237.37N/9.32 MPa	-	[39]
		Cr-coated mild steel (1.2 mm)	-	6127.81N/2.14 MPa	-	[39]
	20 vol% longer fibers (3 mm)	Zn-coated steel (0.7 mm)	-	2400~3300 N	-	[41]
	Longer fibers (3 mm)	Stainless steel 304 (3 mm)	-	4800 N	-	[40, 42]
	7 layers fibers (3 mm)	Stainless steel 304 (2 mm)	-	17.5 MPa	-	[44]
	48 vol% fibers (3 mm)	Stainless steel 304 (2 mm)	S: Metal, grinding; CFRP and metal, acetone	15.7 MPa	Add film (PPS) between two partners	[43]
Bolt	60 wt% (3 mm)	Ti-6Al-4V (3 mm)	B: Ti alloy	~19000 N	-	[24]
Riveting	20 ply layups (2.5mm)	Ti-6Al-4V (2.5 mm)	R: Ti alloy	36700 N	-	[26]
LR			R: Ti-6Al-4V	28500~40300 N	-	[26]
z-pin	CFRP	Ti-6Al-4V	-	14~37 MPa	-	[29]
			-	43000~105000 N	-	[31]
			-	43000~105000 N	-	[30]
	CFRP (5 mm)	Titanium (5 mm)	S: Metal, laser treated	25500~31500 N	-	[32]
	CFRP (11 mm)	Ti-6Al-4V (11 mm)	-	29550~72790 N/ 14.92~36.8 MPa	-	[33]
FSpW	43 wt% woven fibers (2.1 mm)	Mg alloy AZ31 (2 mm)	-	~22.2034 MPa	-	[59]
UW	48 vol% fabric (2 mm)	Al alloy 1050 (1 mm)	-	2460N/25 MPa	-	[38]
AB	67 wt% cross lay-up fibers (0.6 mm)	Al alloy 2017 (0.5 mm)	S: CFRP, acetone; Metal, polish & acetone A: MOS-8	2414 N	-	[50]
MC&AB				4084 N	-	[50]
AB	67 wt% quasi-isotropic lay-up fibers (0.6 mm)			1710 N	-	[50]
MC&AB				3237 N	-	[50]
UW	48 vol% fabric (2 mm)	Al alloy 2024 (1 mm)	-	~33.5 MPa	-	[60]
AB	Cross-ply woven fibers (1.5 mm)	Al alloy 2024 (2.7 mm)	S: CFRP and metal, acetone A: Epoxy resin R: Austenitic steel	3644 N/4480 N (T)	T: Post-curing treatment	[48]
SPR&AB				4475 N/5065 N (T)		[48]
SPR				3392 N		[48]
AB	Angle-ply woven fibers (1.5 mm)			3844 N/4998 N (T)	T: Post-curing treatment	[48]
SPR&AB				5061 N/5852 N (T)		[48]
SPR				3803 N		[48]
SPR	$[0°/45°]_s$ (1.4 mm)	Al alloy 2024 (2.7 mm)	R: Stainless steel	3045.2~3709.6 N	-	[61]
HR	30% short fibers (2 mm)	Al alloy 2024 (2 mm)	-	1300~1600 N	-	[49]
FSpW	50 vol% woven fibers (2.17 mm)	Al alloy 2024 (2 mm)	S: Metal, grinding, R_a=0.84 μm	1276 N/20.2 MPa	-	[56]
			S: Metal, sand blasting, R_a=2~4.5 μm	1908.8 N/31 MPa	-	[56]
		Al alloy 2024 (2 mm); Coated by pure Al	S: Metal, grinding, R_a=0.84 μm	2027.6 N/36.6 MPa	-	[56]
			S: Metal, sand blasting, R_a=2~4.5 μm	2685.4 N/43 MPa	-	[56]

Continued table

	43 wt% woven fibers (2.17 mm)	Al alloy 2024 (2 mm)	S: CFRP and metal, sand blasting	2700~3070 N	Add film (PPS) between CFRP and metal	[58]
				1982~2276 N	-	[58]
FLW	20 wt% short fibers (3 mm)	Al alloy 5052 (2 mm)	-	1000 N	-	[54]
			S: Metal, grinding	2900 N	-	[54, 55]
FSSW	CFRP plate by Mitsubishi Rayon (2 mm)	Al alloy 5052 (2 mm)	-	1504 N/6 or 10.9 MPa	Add film (PA6) between two partners	[62]
IHJ	48 vol% woven fibers (2 mm)	Al alloy 5754 (1 mm)	S: Acetone	7.2 MPa	-	[36]
			S: Plasma treated	~ 8.2 MPa	-	[36]
			S: Corundum blasted	11.1 MPa	-	[36]
			S: Acetone	~12.4 MPa	Add polymer film between two partners	[36]
			S: Corundum	~13.4 MPa		[36]
UW	48 vol% fabric (2 mm)	Al alloy 5754 (1 mm)	-	27.1~31.5 MPa	-	[60]
MCR	53 vol% fibers (1.4 mm)	Al alloy 6024 (3 mm)	-	~2270 N	-	[51]
Riveting	Woven fibers (2 mm)	Al alloy 6060 (2 mm)	R: Stainless steel 304	3980 N	-	[7]
				2730 N	Salt-fog ageing 15 weeks	[7]
AB	68 wt%[0°/±45°/90°]$_s$ (2 mm)	Al alloy 6082 (4 mm)	A: ISOBOND SR 1170	~23000 N	Double lap joint (two CFRP layers)	[25]
Riveting			R: Al	5000 N		[25]
			R: Steel	8250 N		[25]
Riveting & AB			A: ISOBOND SR 1170; R: Al	~27400 N		[25]
Riveting & AB			A: SOBOND SR 1170; S: Steel	~27000 N		[25]
FSBR	30 wt% short fibers (3 mm)	Al alloy 6111 (0.9 mm)	R: Mild steel	3100~3400 N	-	[47]
FSpW	43 wt% woven fibers (2.17 mm)	Al alloy 6181 (1, 1.5 mm)	-	2107~3523 N	Double lap joint (two metal layers)	[57]
AB	T300-3K (tube)	Al alloy 7075 (bar)	A: DP460 S: CFRP and metal: clean	8735 N	-	[12, 13]
UVAB				12279 N	Load ultrasonic vibration along radial direction	[12,13]
				13336 N	Load ultrasonic vibration along axial direction	[12,13]
AB	[±45°/0°/90°]$_s$ (2.1 mm)	Al alloy 7075 (3.224 mm)	A: FM73	453 MPa	Double lap joint (two CFRP layers)	[27]
			A: EA9394S	67.1 MPa		[27]
Bolt			B: Steel	162 MPa		[27]
Bolt&AB			A: FM73; B: Steel	440 MPa		[27]
			A: EA9394S; B: Steel	192 MPa		[27]
RW	47.3 vol% woven fibers（10 layers）	Al alloy 7075 (3 mm)	S: Metal, standard surface treatment for AB	>20 MPa	-	[35]
LJ	22 vol% fibers (3.5 mm)	Al alloy 7075 (2 mm)	-	8.5 MPa	-	[46]
			S: Metal, laser Surfi-Sculpt	18.5~39 MPa	-	[46]

Appendix B: Abbreviations

AB	Adhesive bonding
BR	Blind riveting
CFRP	Carbon fiber-reinforced polymer
CMT	Cold metal transfer
EBM	Electron beam melting
FLW	Friction lap welding
FR	Friction riveting
FSBR	Friction stir blind riveting
FSpW	Friction spot welding
FSSW	Friction stir spot welding
HMC	Hole mechanical clinching
HR	Hot riveting
IHJ	Induction heated joining
LJ	Laser joining
LR	Laser riveting
MC	Mechanical clinching
MCR	Mechanical clinching with reshaping
RW	Resistance welding
SPR	Self-pierce riveting
UVAB	Ultrasonic vibration-assisted adhesive bonding
UW	Ultrasonic welding

References

1 Soutis C. *Progress in Aerospace Sciences*[J], 2005, 41: 143
2 Du Shanyi. *Acta Materiae Compositae Sinica*[J], 2007, 24(1): 1 (in Chinese)
3 Jaeschke P, Wippo V, Suttmann O *et al. Journal of Laser Applications*[J], 2015, 27(S2): 9004.
4 Cao Chunxiao. *Acta Aeronautica et Astronautica Sinica*[J], 2008, 29(3): 701 (in Chinese)
5 Malinowski P, Wandowski T, Ostachowicz W. *Structural Health Monitoring*[J], 2015, 14(4): 332
6 Zhang D W, Zhang Q, Fan X G *et al. Rare Metal Materials and Engineering*[J], 2018, 47(12): 3686
7 Fiore V, Calabrese L, Proverbio E *et al. Composites Part B*[J], 2017, 108: 65
8 Wagner J, Wilhelm M, Baier H *et al. International Journal of Advanced Manufacturing Technology*[J], 2014, 75: 1103
9 Ashcroft I A, Hughes D J, Shaw S J. *Assembly Automation*[J], 2000, 20(2): 150
10 Gotoh K, Kikuchi S. *Colloid and Polymer Science*[J], 2005, 283(12): 1356
11 Zhang K, Yang Z, Li Y. *International Journal of Adhesion & Adhesives*[J], 2013, 46: 7
12 Wang Hui, Hao Xufei, Hua Lin *et al. Journal of Huangzhong University of Science and Technology*[J], 2016, 44(5): 127 (in Chinese)
13 Wang H, Hao X F, Zhou H M *et al.* J*ournal of Adhesion Science and Technology*[J], 2016, 30(17): 1842
14 Chishti M, Wang C H, Thomson R S *et al*. *Composite Structures*[J], 2012, 94(2): 643
15 Wang Danyong, Wen Weidong, Cui Haitao. *Acta Materiae Composite Sinica*[J]. 2005, 22(3): 168 (in Chinese)
16 Jiang Yunpeng, Yue Zhufeng. *Acta Materiae Composite Sinica*[J], 2005, 22(4): 177 (in Chinese)
17 Xiao Y, Ishikawa T. *Composites Science and Technology*[J], 2005, 65: 1022
18 Xiao Y, Ishikawa T. *Composites Science and Technology*[J], 2005, 65: 1032
19 Zhao Libin, Xu Jifeng. *Analysis Method of Advanced Composite Material Joining Structure*[M]. Beijing: Beihang University Press, 2015 (in Chinese)
20 Caccese V, Mewer R, Vel S S. *Engineering Structures*[J], 2004, 26: 895
21 Scattina A, Roncato D, Belingardi G *et al. Composite Structures*[J], 2015, 134: 378
22 McCarthy M A, Lawlor V P, Stanley W F. *Journal of Composite Materials* [J], 2005, 39(9): 799
23 Li J, Li Y, Zhang K *et al. Fatigue & Facture of Engineering Materials & Structures*[J], 2015, 38: 1359
24 Li J, Zhang K, Li Y *et al. Tribology International*[J], 2016, 93: 151
25 Marannano G, Zuccarello B. *Composites: Part B*[J], 2015, 71: 28
26 Kashaev N, Ventzke V, Riekehr S *et al. Materials and Design*[J], 2015, 81: 73
27 Kweon J H, Jung J W, Kim T H *et al. Composite Structures*[J], 2006, 75: 192
28 Ucsnik S, Scheerer M, Zaremba S *et al. Composites: Part A*[J], 2010, 41: 369
29 Giandomenico V D, Joesbury A, Millán M P. *Poster Book 2013-2014 of EPSRC Centre for Innovative Manufacturing in Composites*[C]. Nottingham: EPSRC Center for Innovative Manufacturing in Composites, 2014: 23
30 Cook L, Giandomenico V D. *Poster Book 2014-2015 of EPSRC Centre for Innovative Manufacturing in Composites* [C]. Nottingham: EPSRC Center for Innovative Manufacturing in Composites, 2015: 54
31 Giandomenico V D. *Poster Book 2014-2015 of EPSRC Centre for Innovative Manufacturing in Composites*[C]. Nottingham: EPSRC Center for Innovative Manufacturing in Composites, 2015: 56
32 Parkes P N, Butler R, Meyer J *et al. Composite Structures*[J], 2014, 118: 250
33 Wang X, Ahn J, Lee J *et al*. *Materials and Design*[J], 2016, 101: 188
34 Tian Yingchao, Qu Wenqing, Zhang Zhiyong *et al. Aeronautical Manufacturing Technology*[J], 2011(9): 82 (in Chinese)
35 Ageorges C, Ye L. *Journal of Thermoplastic Composite Materials*[J], 2001, 14: 449
36 Mitschang P, Velthuis R, Emrich S *et al. Journal of Thermoplastic Composite Materials*[J], 2009, 22: 449
37 Balle F, Huxhold S, Emrich S *et al. Advanced Engineering*

Materials[J], 2013, 15(9): 837

38 Balle F, Wagner G, Eifler D. *Materialwissenschaft Und Werkstofftechnik*[J], 2007, 38(11): 934

39 Tan Xianghu, Shan Jiguo, Ren Jialie. *Acta Metallurgica Sinica*[J], 2013, 49(6): 751 (in Chinese)

40 Jung K W, Kawahito Y, Katayama S. *Science and Technology of Welding and Joining*[J], 2011, 16(8): 676

41 Jung K W, Kawahito Y, Takahashi M *et al. Materials and Design*[J], 2013, 47: 179

42 Katayama S, Kawahito Y. *Industrial Laser Solutions*[J], 2014, 29(4): 22

43 Wang Feiya, Jiao Junke, Wang, Qiang *et al*. *Proceedings of the 16th National Conference on Special Processing of China*[C]. Xiamen: Mechanical Engineering Society, 2015: 134 (in Chinese)

44 Jiao J, Wang Q, Wang F *et al*. *Journal of Materials Processing Technology*[J], 2017, 240: 362

45 Tan X, Zhang J, Shan J *et al. Composites: Part B*[J], 2015, 70: 35

46 Zhang Z, Shan J, Tan X *et al. International Journal of Advanced Manufacturing Technology*[J], 2017, 90: 3465

47 Min J, Li Y, Li J *et al. International Journal of Advanced Manufacturing Technology*[J], 2015, 76: 1403

48 Di Franco G, Fratini L, Pasta A. *International Journal of Adhesion & Adhesives*[J], 2013, 41: 24

49 Zhang Weijun. *Thesis for Master*[D]. Xi'an: Xi'an Jiaotong University, 2015 (in Chinese)

50 Huang Z, Sugiyama S, Yanagimoto J. *Journal of Materials Processing Technology*[J], 2013, 213: 1864

51 Lambiase F, Ko D C. *Composite Structures*[J], 2017, 164: 180

52 Zhao S D, Xu F, Guo J H *et al. Journal of Materials Processing Technology*[J], 2014, 214: 2134

53 Lee S H, Lee C J, Lee K H *et al. Advanced in Mechanical Engineering*[J], 2015, 6: 1

54 Nagatsuka K, Yoshida S, Tsuchiya A *et al. Composites: Part B* [J], 2015, 73: 8.

55 Kimiaki N, Xiao B, Atsuki T *et al*. *Transaction of JWRI*[J], 2015, 44(1): 9

56 Goushegir S M, dos Santos J F, Amancio-Filho S T. *Materials and Design*[J], 2014, 54: 196

57 Esteves J V, Goushegir S M, dos Santos J F *et al. Materials and Design*[J], 2015, 66: 437

58 André N M, Goushegir S M, dos Santos J F *et al*. *Composites Part B*[J], 2016, 94: 197

59 Amancio-Filho S T, Bueno C, dos Santos J F *et al. Materials Science and Engineering A*[J], 2011, 528: 3841

60 Wagner G, Balle F, Eifler D. *Advanced Engineering Materials* [J], 2013, 15(9): 792

61 Franco G D, Fratini L, Pasta A *et al*. *International Journal of Material Forming*[J], 2013, 6: 137

62 Tanaka K, Teramura T, Katayama T *et al. WIT Transactions on the Built Environment*[J], 2016, 166: 391

碳纤维增强树脂基复合材料和金属材料连接技术综述：应用和展望

张大伟[1]，张　琦[1]，樊晓光[2]，赵升吨[1]

(1. 西安交通大学 现代设计及转子轴承系统教育部重点实验室，陕西 西安 710049)

(2. 西北工业大学 凝固技术国家重点实验室，陕西 西安 710072)

摘　要：复合材料（如碳纤维增强树脂基复合材料(CFRP)）和金属材料（如钢、铝合金、钛合金等）混合结构有效实现轻量化，并保证结构强度，其应用在飞机、汽车、船舶中迅速增加。先进的基于塑性变形连接的CFRP-金属混合接头重量轻、强度高、适用于复杂多样环境，具有广泛的应用前景。本文综述了不同CFRP和金属连接技术应用范围、接头强度等方面的研究成果。指出了高性能、轻量化、高可靠性的CFRP-金属混合接头进一步研究发展所要解决的问题。

关键词：碳纤维增强树脂基复合材料；铝合金；钢；钛合金；铌合金；接头强度

作者简介：张大伟，男，1982 年生，博士，副教授/博导，西安交通大学机械工程学院，陕西 西安 710049，电话：029-82668607，E-mail: zhangdawei2000@mail.xjtu.edu.cn